Enhanced Resolution Imaging From Irregular Samples

David S. Early, David G. Long

Electrical and Computer Engineering Department, Brigham Young University
459 Clyde Building, Provo, Utah 84602
(801) 378-4383 fax: (801) 378-6586 long@ee.byu.edu

Abstract - **This paper considers techniques for creating enhanced resolution images from irregular samples, with specific application to imaging from scatterometers. Using previously established irregular sampling theory, and developing the idea of sub-band limited Banach space, we show that frequency content in attenuated sidelobes can be recovered using resolution enhancement techniques, thus taking advantage of the high frequency content of measurements made with imperfect low pass aperture filters. We briefly compare and contrast the performance of additive ART, multiplicative ART and the Scatterometer Image Reconstruction (SIR) (a derivative of multiplicative ART) algorithms with and without noise.**

I. INTRODUCTION

A theory for resolution enhancement from irregular samples is presented. The theory and techniques are illustrated for enhanced resolution ERS-1 scatterometer imagery. First, a theory of image reconstruction from irregular samples and the equivalence of the algebraic reconstruction technique (ART) and this theory are discussed. We demonstrate that reconstruction can recover sidelobe information and consider the practical use of the theory with the addition of noise to the reconstruction. We discuss scatterometer image reconstruction (SIR), a derivative of multiplicative ART tailored to reduce the influence of noise on enhanced resolution image reconstruction from scatterometer data [6].

II. SYSTEM MODEL

While this theory is developed around a model of the surface response that describes the microwave backscatter from a point, it is generally applicable. We desire to make images of the backscatter from ERS-1 scatterometer measurements. We model the radar backscatter (σ^o) from the surface as a function of location with the backscatter's incidence angle dependence suppressed.

Let $f(x, y)$ be the function that gives the backscatter from a point (x, y) on the surface. The measurement system can be modeled by

$$z = Hf + \text{noise} \tag{1}$$

where H is an operator that models the measurement system (aperture filtering and sample spacing), f is the true surface function, and z represents measurements of σ^o made by the instrument. For resolution enhancement, we are interested in the inverse problem:

$$\hat{f} = \hat{H}^{-1} z \tag{2}$$

where $\hat{f}$ is an estimate of f from the measurements z. The inverse of the operator H, $\hat{H}^{-1}$, is exact only if the measurements are noise free and H is invertible, in which case $\hat{f} = f$.

Real-life sampling usually involves a non-ideal sampler with a finite aperture which low-pass filters the data. The aperture functions may have frequency nulls that result in information which can not be recovered. However if suitably sampled and processed, information in the aperture frequency response sidelobes can be recovered if the signal-to-noise ratio (SNR) is sufficiently high.

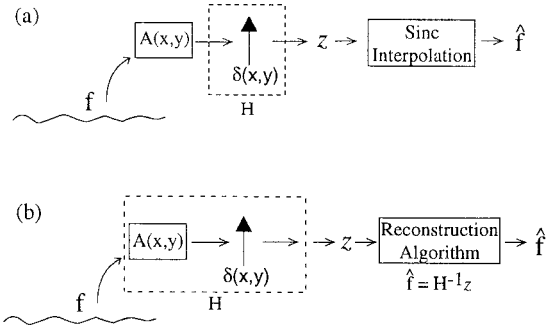

Figure 1. *Block diagram illustrating sampling and signal recovery. The original surface, f, is filtered by the system aperture function, $A(x, y)$, and sampled to obtain the measurements z. In (a), the signal is uniformly sampled. The surface function is recovered using low pass filtering which inverts only the sampling. In (b), the operator inverted, denoted by H and the dotted box, includes both the aperture function and the sampling. Sampling is dense and may be irregular.*

The traditional approach to sampling and reconstruction is based on the Nyquist sampling theorem which states that a band limited function can be completely reconstructed from regularly spaced samples if the sample rate exceeds the Nyquist sample rate of twice the maximum frequency in the signal. The reconstruction is done with a simple low pass filter consistent with the sampling. The filter is equivalent to using a *sinc* function as an interpolating function (see Fig. 1). When possible, the aperture function is designed to act as a prefilter to eliminate high frequency components of the signal that might otherwise cause aliasing in the reconstructed signal. Such an approach was used with the ERS-1 scatterometer design: A desired sample spacing of 25 km dictated an aperture function that filters wavelengths smaller than 50 km to minimize aliasing.

Because the aperture function is non-ideal, if the data is over-sampled at least some of the higher frequency content of the original signal can be recovered using a reconstruction algorithm which inverts both the sampling and aperture functions [see Fig. 1(b)].

III. IRREGULAR SAMPLING THEORY

In this section we consider irregular sampling and reconstruction. We are interested in irregular sampling because we can combine multiple passes of a scatterometer to achieve a closely spaced irregular sample grid [4].

Gröchenig analyzed the irregular sampling problem [1]. He presented a lemma which can be stated as follows: Let A be a bounded operator on a Banach space B such that $\|I - A\|' < 1$ (I is the Identity Operator), where $\|\cdot\|'$ denotes the operator norm on B. Then A is invertible on B and $A^{-1} = \sum_{n=0}^{\infty}(I - A)^n$. Moreover, every $f \in B$ can

be reconstructed by the iteration

$$\phi_0 = Af$$
$$\phi_{n+1} = \phi_n - A\phi_n$$
$$f = \sum_{n=0}^{\infty} \phi_n$$

with convergence in B. The operator A which includes the sampling and aperture functions must be bounded with $\|I - A\|' < 1$.

Gröchenig showed that if f is band limited on a Banach space and sampling is δ-dense with $\delta \cdot \omega < ln(2)$ where ω represents the highest frequencies present in f, f can be reconstructed from its samples using this algorithm [1]. Experimental results for the ERS-1 scatterometer when several days of data are considered show that in the polar regions, the sampling sets are δ-dense with $\delta = 10$ km to 13 km [4]. The best resolution recovery is thus approximately 30 km, a value consistent with experimental results [4].

It can be shown that Gröchenig's Algorithm is functionally equivalent to the additive algebraic reconstruction technique (ART), a well-established image reconstruction technique [3]. Block additive ART can be written as [2]

$$a_{n+1}^j = a_n^j + \frac{\sum_i (s_i - p_i) h_{ij}}{\sum_i h_{ij}} \quad (3)$$

where a represents the image to be estimated, a_n is the n^{th} iterative estimate of a, j is the pixel index and i is the measurement index. The essence of this equation is that all measurements that touch a pixel a^j are summed and normalized to create the per pixel update value. Eq. (3) can be written as

$$a_{n+1} = a_n + \mathcal{H}(a - a_n) \quad (4)$$

where the a's are now vectors with a being the 'true' image, a_n the nth iterative estimate of a and $\mathcal{H} = H'H$ is an $N \times N$ matrix operator equivalent to Gröchenig's A [3]. H incorporates both the sampling and the aperture function.

While Gröchenig was primarily interested in low-pass function, we are interested in signals sampled by an aperture function with side lobes and nulls. We thus consider the sub-band limiting scheme illustrated in Fig. 2. It can be shown that such a sub-band limited space defined in Fig. 2(a) is a Banach space [3].

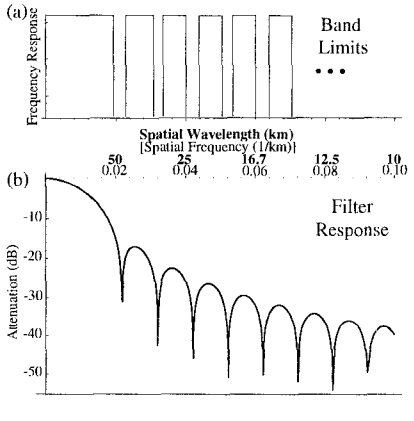

Figure 2. *(a) A band limiting scheme that delimits nulls in the filter response in (b). (b) Frequency response of the ERS-1 scatterometer.*

In the following discussion we assume that the sample spacing is adequate (δ-dense) for recovering the desired original and deal strictly with aperture function affects on invertibility. We define the domain of H to be $u \in B^2(\Omega')$ which consists of all functions with a sub-band limited frequency response as illustrated in Figure 2(a). The low pass characteristics of the aperture function built into the operator H indicate that certain frequencies of an arbitrary input are nulled out and therefore unrecoverable in any reconstruction. By setting the domain $B^2(\Omega')$ to be exclusively functions without those frequencies, no information is lost for $v = Hu$, though v may have attenuated frequency components. Then, $u' = H'v = H'Hu \in B^2(\Omega')$ is also in the original Banach space. Thus, $\mathcal{H} = H'H$ is a bounded operator on the sub-band limited Banach space, meeting the first requirement of Gröchenig's Lemma. Further, $\mathcal{H}$ will be invertible on this Banach space. It follows that Eq. (4) represents a valid algorithm for the *complete* recovery of the original vector a within Banach space $B^2(\Omega')$. Note, however, that *complete* recovery is only possible if the original function is contained in the Banach space spanned by the operator inverse $\mathcal{H}^{-1}$, i.e., $B^2(\Omega')$. Otherwise, as discussed below, the result is an approximation of the original function.

IV. PRACTICAL APPLICATION

While $\mathcal{H}$ is a valid operator for Gröchenig's algorithm for function which is band-limited or sub-band-limited, in application the surface function may not be sub-band limited. The original function can only be recovered in the sub-bands over which $\mathcal{H}$ is invertible. Ideally, we would modify or reduce the space to correspond to a band-limited form. However, it is frequently impractical, from an algorithmic and computational standpoint, to reduce the problem to such a form. Instead, for practical application we use regularization of $\mathcal{H}$ to insure its invertibility over the full space. The ART algorithms implicitly include regularization. Block additive ART is a least squares solution to the inverse problem in Eq. (2) while multiplicative ART with damping is a maximum entropy estimate in the limit [2][5]. Thus, even if the complete original function is unrecoverable, ART algorithms provide good estimates of the original function.

The Scatterometer Image Reconstruction (SIR) algorithm is a modified multiplicative ART algorithm specifically designed for scatterometer data reconstruction [4]. The SIR update has square root damping and includes a non-linearity to minimize the effects of noise and reaches the maximum entropy solution in the limit [6].

The results of additive ART, multiplicative ART and SIR are similar in the noiseless case. However, because of noise in the measurements, none of the reconstruction algorithms can be run for more than a few dozen iterations so the theoretical limits may not be reached. Nevertheless, as will be shown the algorithms provide good resolution enhancement with only limited iterations. The limited iteration results are *approximations* of the least squares or maximum entropy solution. Experimental data demonstrates that even highly attenuated frequency components are effectively recovered with finite iterations.

In order to illustrate and compare the ART and the SIR algorithm each are applied to a simple 1-D signal. A *sinc* function was chosen since it readily shows the frequency domain reconstruction from the various methods. The test signal is sampled with an irregular sampling grid. A rectangular aperture was chosen for convenience and its utility for demonstrating sidelobe recovery. The relationship between the spectrum of the aperture function and the test signal is illustrated in Fig. 3. The rectangular aperture for this study was chosen so that the first side

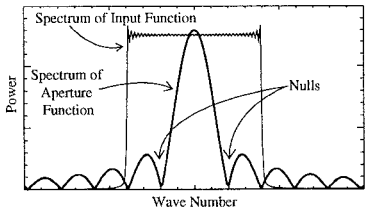

Figure 3. *Illustration of the overlay of the test signal spectrum (light) with the frequency response of the aperture function (bold).*

lobe of the aperture is inside the spectrum of the test signal as illustrated in Fig. 3, allowing the reconstruction of the attenuated and nulled frequencies within the side lobe to be easily evaluated. For each algorithm, a noisy case is also considered. Following the scatterometer noise model, multiplicative Gaussian noise with a K_p of 5% is added to the test signal.

Figure 4 illustrates the spectra of the output from Multiplicative ART and SIR at 25 and 100 iterations for both noiseless and noisy cases. (Both additive and multiplicative ART produce similar results for these cases.) While the noiseless case shows very good spectral recovery for just a few iterations, the performance of the ART algorithms in the presence of noise is significantly degraded. After 100 iterations the energy in the noise outside the desired band is increasing rapidly for the ART algorithm.

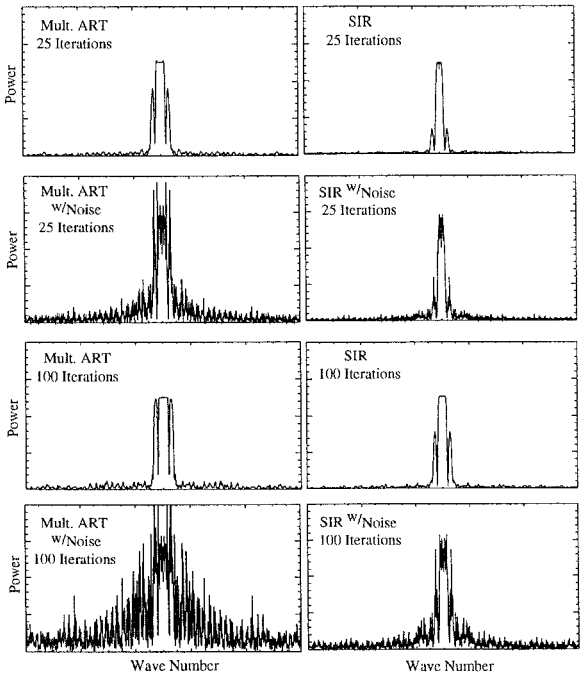

Figure 4. *Spectra of multiplicative ART and SIR with noiseless and noisy measurements in the simulation.*

In the noiseless case the signal is completely recovered with sufficient iterations for all of the algorithms. The poor performance of ART in the presence of noise originally motivated the development of SIR [6]. For SIR, the multiplicative scale factor is damped so that large scale factors do not overly magnify the noise at any one iteration, slowing the reconstruction but minimizing the effects of the noise. This is evident in the first sidelobe of the SIR estimate which, while enhanced, is not as noisy as it is for ART.

Figure 5 compares the error performance of the three algorithms in the simulation. To compute the total squared error shown, the output at each iteration is subtracted from the original test function and the difference squared and summed. The noisy cases for multiplicative and additive ART show greater error with increasing it-

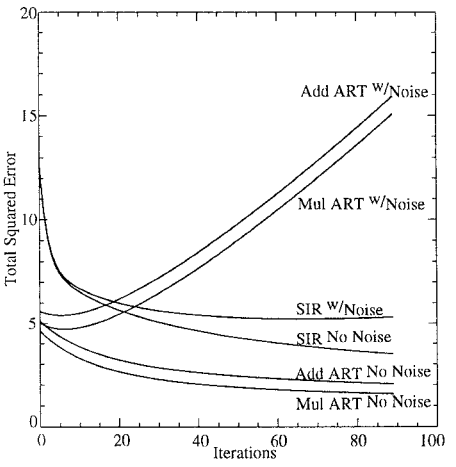

Figure 5. *Cumulative squared error between the output of the algorithms for various iterations and noise.*

erations after a brief initial decrease. Even though the total squared error is low in the initial iterations for the ART algorithms, a minimum number of iterations (about 30) is required to generate acceptable resolution enhancement, in which case SIR begins to perform better than the ART algorithms. SIR is also convergent to a lower total error than the ART algorithms which are nonconvergent for noisy measurements. The curves in Fig. 5 do not converge to zero because of the nulls in the aperture function. The corresponding frequencies are unrecoverable and result in some minimum error level between the original signal and the algorithm outputs. Based on Fig. 5 we conclude that SIR performs better when noise is present. Noting that the SIR algorithm also recovers the incidence angle response [6], we conclude that it is better suited for application to scatterometer data than an ART algorithm.

V. SUMMARY

Gröchenig's results suggest that a sub-bandlimited signal can be recovered from irregular samples. By using multiple passes of ERS-1 scatterometer data, an irregular δ-dense sampling grid of measurements is produced. Using a reconstruction algorithm such as ART or SIR permits resolution enhancement in excess of the Nyquist rate and the aperture function frequency response for a single pass.

REFERENCES

[1] K. Gröchenig, "Reconstruction Algorithms in Irregular Sampling," *Mathematics of Computation*, vol. 59, no. 199, pp. 181–194, 1992.

[2] Y. Censor, "Finite series-expansion reconstruction methods," *Proc. IEEE*, vol. 71, no. 3, pp. 409–419, March 1983.

[3] D.S. Early and D.G. Long, "Enhanced Resolution Imaging from Irregular Samples," Submitted to, *IEEE Trans. Geosc. Remote Sens.*, 1997.

[4] D.S. Early and D.G. Long, "Error and Resolution Characteristics of the SIRF Resolution Enhancement Algorithm," *Proc. IGARSS*, Lincoln, Nebraska, pp. 124–126, 1996.

[5] T. Elfving, "On Some Methods for Entropy Maximization and Matrix Scaling," *Linear Algebra and its Applications*, no. 34, pp. 321–339, 1980.

[6] D.G. Long, P. Hardin, and P. Whiting, "Resolution Enhancement of Spaceborne Scatterometer Data," *IEEE Trans. Geosci. Remote Sens.*, vol. 31, pp. 700–715, 1993.